

RESEARCH LETTER

10.1002/2017GL075043

Key Points:

- Published high-stress rock deformation data are reanalyzed by rigorous statistical analysis
- Our inversion results yield significant nonuniqueness in the flow law parameters for low-temperature plasticity
- The diversity of the yield strength of oceanic lithosphere has bearings on the origin of plate tectonics

Supporting Information:

- Supporting Information S1

Correspondence to:

C. Jain,  
 chhavi.jain@yale.edu

Citation:

Jain, C., Korenaga, J., & Karato, S.-I. (2017). On the yield strength of oceanic lithosphere. *Geophysical Research Letters*, 44, 9716–9722. <https://doi.org/10.1002/2017GL075043>

Received 21 JUL 2017

Accepted 25 SEP 2017

Accepted article online 2 OCT 2017

Published online 14 OCT 2017

On the Yield Strength of Oceanic Lithosphere

Chhavi Jain<sup>1</sup>, Jun Korenaga<sup>1</sup>, and Shun-ichiro Karato<sup>1</sup>

<sup>1</sup>Department of Geology and Geophysics, Yale University, New Haven, CT, USA

**Abstract** The yield strength of oceanic lithosphere determines the mode of mantle convection in a terrestrial planet, and low-temperature plasticity in olivine aggregates is generally believed to govern the plastic rheology of the stiffest part of lithosphere. Because, so far, proposed flow laws for this mechanism exhibit nontrivial discrepancies, we revisit the recent high-pressure deformation data of Mei et al. (2010) with a comprehensive inversion approach based on Markov chain Monte Carlo sampling. Our inversion results indicate that the uncertainty of the relevant flow law parameters is considerably greater than previously thought. Depending on the choice of flow law parameters, the strength of oceanic lithosphere would vary substantially, carrying different implications for the origin of plate tectonics on Earth. To reduce the flow law ambiguity, we suggest that it is important to establish a theoretical basis for estimating macroscopic stress in high-pressure experiments and also to better utilize marine geophysical observations.

1. Introduction

The existence of plate tectonics is unique to Earth in our solar system. The mantle of a terrestrial planet like Earth generally has strongly temperature-dependent viscosity (e.g., Karato and Wu, 1993), and such rheology is expected to result in stagnant lid convection (Solomatov, 1995). The wholesale subduction of the top boundary layer (or the lithosphere) on Earth requires that the lithosphere has to be considerably weaker than indicated by temperature-dependent viscosity. To investigate potential mechanisms that can reduce lithospheric strength, we must first have a good understanding of how strong the undamaged lithosphere actually can be. The lithosphere spans over a wide range of temperature, from ~273 K at the surface to ~1500 K at its base. At shallow depths, rocks deform by brittle failure, but in deeper parts of the lithosphere, they flow plastically (Kohlstedt et al., 1995). Olivine is the primary constituent and usually the weakest phase of the lithospheric mantle, and its low-temperature and high-stress plasticity, described by glide-controlled dislocation creep, is often used to define the ductile yield strength of oceanic lithosphere.

In the low-temperature plasticity regime, strain rate increases exponentially with stress, as represented by the following steady state flow law (Karato, 2008, chap. 9):

$$\dot{\epsilon}_p = A\sigma^2 \exp\left(-\frac{E + PV}{RT} \left[1 - \left\{\frac{\sigma}{\sigma_p}\right\}^p\right]^q\right), \tag{1}$$

where  $\dot{\epsilon}_p$  is strain rate in  $s^{-1}$ ,  $A$  is the scaling coefficient,  $\sigma$  is deviatoric stress in megapascal,  $T$  is absolute temperature in kelvin,  $P$  is pressure in pascal,  $E$  is activation energy in  $J\ mol^{-1}$ ,  $V$  is activation volume in  $m^3\ mol^{-1}$ ,  $\sigma_p$  is the Peierls stress in megapascal,  $R$  is the gas constant, and exponents  $p$  and  $q$  are constants. The Peierls stress is the stress required for dislocations to overcome the Peierls potential without thermal activation and glide. The Peierls potential function, and consequently, the Peierls stress depend on the shear modulus  $G$  of the material under consideration and vary with pressure. The exponents  $p$  and  $q$  depend on the shape of the Peierls potential. Theoretical considerations suggest that  $0 \leq p \leq 1$  and  $1 \leq q \leq 2$  (e.g., Frost and Ashby, 1982, chap. 2; Kocks et al., 1975, chap. 5), and each combination of  $p$  and  $q$  corresponds to a unique set of flow law parameters. The  $\sigma^2$  term represents the dependence of strain rate on dislocation density (e.g., Karato, 2008, chap. 9), where the stress exponent of 2 is based on a simple theory (Karato, 2008, chap. 5). However, a stress exponent of ~1.4 has been obtained experimentally for olivine (e.g., Karato and Jung, 2003), which suggests some complications in the dislocation interaction in that mineral. Because we do not fully understand what causes this difference, and because this value does not affect our conclusions significantly, we choose to use the canonical value of 2 for the exponent.

A few experimental studies have been conducted to determine flow law parameters for low-temperature plasticity in olivine, but their estimates do not agree with each other. For example, Evans and Goetze (1979) obtained  $\sigma_p = 9.1$  GPa and  $E = 502$  kJ mol<sup>-1</sup> at ambient pressure assuming the exponents  $p = 1$  and  $q = 2$ , whereas Raterron et al. (2004) obtained  $\sigma_p = 15.4$  GPa and  $E = 564$  kJ mol<sup>-1</sup> at  $\sim 9$  GPa using  $p = 2/3$  and  $q = 2$ . Both studies used a simplified flow law in which the  $\sigma^2$  factor was neglected. By assuming the flow law suggested by Evans and Goetze (1979), Kawazoe et al. (2009) estimated an activation volume of  $\sim 30$  cm<sup>3</sup> mol<sup>-1</sup>. Mei et al. (2010) retained the  $\sigma^2$  factor but did not consider pressure effects. By assuming  $p = 1/2$  and  $q = 1$ , the linear least squares regression of their data yielded  $\sigma_p = 5.9$  GPa and  $E = 320$  kJ mol<sup>-1</sup>. More recent studies, such as Long et al. (2011) and Proietti et al. (2016), suggest more divergent flow laws for low-temperature plasticity in olivine aggregates.

The discrepancy between these results may originate in the use of different exponents ( $p, q$ ), but such a possibility was not considered by most of these studies. This may be because the analysis of Frost and Ashby (1982) had shown that the choice of exponents did not significantly affect model predictions under laboratory conditions. However, extrapolation to geological conditions could produce considerably different predictions with different pairs of  $p$  and  $q$ . This possibility needs to be explored, and, if true, the exponents most suitable for olivine under upper mantle conditions must be identified.

The aim of our study is, therefore, to revisit published experimental data with the fully nonlinear constitutive equation for low-temperature plasticity (equation (1)), which includes the  $\sigma^2$  term and all pressure effects. We note, however, that strain rates are not well constrained in microindentation experiments of Evans and Goetze (1979) and that steady state was not confirmed in the experiments conducted by Raterron et al. (2004). Strain rates observed by Kawazoe et al. (2009) indicate a significant contribution of dislocation creep. Studies by Long et al. (2011) and Proietti et al. (2016) explored only a narrow range of pressure (4.1–5.3 GPa) and temperature (room temperature), respectively, thus being unlikely to resolve the corresponding flow law parameters given the high degree of nonlinearity in equation (1). In comparison, Mei et al. (2010) deformed their samples over a wider range of experimental conditions, thereby providing the most useful data set for our analysis. We thus focus on reanalyzing the high-pressure data of Mei et al. (2010) using the inversion technique developed by Korenaga and Karato (2008), which is based on Bayesian statistics and implemented by the Markov chain Monte Carlo (MCMC) sampling. This MCMC-based inversion can handle highly nonlinear models such as equation (1) with no difficulty. Using this technique, we compare flow law parameters for low-temperature plasticity estimated with various combinations of ( $p, q$ ). The geophysical significance of our results is discussed on the basis of corresponding lithospheric yield stresses.

## 2. Method

For the influence of pressure on  $\sigma_p$ , we adopt the following relationship proposed by Kawazoe et al. (2009):

$$\sigma_p(P) = \sigma_p^0 \left( 1 + \frac{G'P}{G_0} \right), \quad (2)$$

where  $\sigma_p^0$ ,  $G_0$ , and  $G'$  are the Peierls stress, the shear modulus, and its pressure derivative, respectively, at ambient pressure. The elastic parameters are experimentally determined as  $G_0 = 77.4$  GPa and  $G' = 1.61$  (Liu et al., 2005). As  $\dot{\epsilon}_p$ ,  $\sigma$ ,  $T$ , and  $P$  are state variables that are measured in the laboratory,  $A$ ,  $\sigma_p^0$ ,  $E$ , and  $V$  are the flow law parameters to be estimated by inversion. We consider all of the following combinations of ( $p, q$ ): (1, 1), (1, 2), (3/4, 4/3), (2/3, 3/2), (1/2, 2), and (1/2, 1) (Frost and Ashby, 1982, Figure 2.3).

The MCMC algorithm originally implemented by Korenaga and Karato (2008) was later improved by Mullet et al. (2015), and we use this modified algorithm in our study. We refer to these studies for a detailed explanation of this inversion technique. The model space to be explored by the MCMC algorithm is defined by providing an a priori range for each model parameter. The resulting posterior probability distribution can then be used to compute various statistical estimators, such as mean and covariance. We assume the following a priori bounds:  $4 \leq \sigma_p^0 \leq 10$  GPa,  $10 \leq E \leq 1000$  kJ mol<sup>-1</sup>, and  $0 \leq V \leq 40$  cm<sup>3</sup> mol<sup>-1</sup>, which broadly cover the values of these parameters estimated by some previous studies mentioned in section 1, and use the mean and standard deviation of each parameter to summarize our results.

**Table 1**  
Results of Inversion of Data of Mei et al. (2010) for the Comprehensive Flow Law of Low-Temperature Plasticity (Equation (1))

$p$	$q$	$\sigma_p^0$	$E$	$V \times 10^{4a}$	$\log_{10}(A)$	$\chi_s^2/N$
(a) $0 \leq V \leq 40 \text{ cm}^3 \text{ mol}^{-1}$						
1	1	$4.51 \pm 0.06$	$185.9 \pm 13.4$	$2 \pm 2$	$-7.59 \pm 0.16$	$3.36 \times 10^3$
1	2	$6.20 \pm 0.12$	$225.3 \pm 14.0$	$3 \pm 4$	$-7.69 \pm 0.23$	$2.61 \times 10^3$
3/4	4/3	$5.29 \pm 0.09$	$249.5 \pm 15.6$	$3 \pm 4$	$-7.66 \pm 0.28$	$2.75 \times 10^3$
2/3	3/2	$5.73 \pm 0.11$	$289.5 \pm 17.1$	$3 \pm 4$	$-7.69 \pm 0.35$	$2.53 \times 10^3$
1/2	2	$7.32 \pm 0.19$	$452.4 \pm 25.6$	$8 \pm 118$	$-7.78 \pm 0.67$	$2.22 \times 10^3$
1/2	1	$4.79 \pm 0.08$	$294.6 \pm 18.5$	$3 \pm 3$	$-7.63 \pm 0.37$	$2.84 \times 10^3$
$p$	$q$	$\sigma_p^0$	$E$	$V$	$\log_{10}(A)$	$\chi_s^2/N$
(b) $-40 \leq V \leq 40 \text{ cm}^3 \text{ mol}^{-1}$						
1	1	$4.72 \pm 0.07$	$222.4 \pm 13.4$	$-3.91 \pm 0.69$	$-7.06 \pm 0.19$	$2.44 \times 10^3$
1	2	$6.58 \pm 0.14$	$255.3 \pm 14.8$	$-3.98 \pm 0.81$	$-7.26 \pm 0.26$	$1.98 \times 10^3$
3/4	4/3	$5.59 \pm 0.11$	$285.4 \pm 16.5$	$-4.57 \pm 0.89$	$-7.22 \pm 0.31$	$2.11 \times 10^3$
2/3	3/2	$6.09 \pm 0.13$	$324.8 \pm 18.9$	$-5.00 \pm 1.04$	$-7.29 \pm 0.39$	$1.92 \times 10^3$
1/2	2	$7.90 \pm 0.22$	$488.3 \pm 27.2$	$-7.02 \pm 1.55$	$-7.42 \pm 0.71$	$1.78 \times 10^3$
1/2	1	$5.05 \pm 0.09$	$338.9 \pm 19.6$	$-5.53 \pm 1.05$	$-7.19 \pm 0.41$	$2.10 \times 10^3$

Note. Two different a priori bounds on  $V$  are explored: (a)  $0 \leq V \leq 40 \text{ cm}^3 \text{ mol}^{-1}$  and (b)  $-40 \leq V \leq 40 \text{ cm}^3 \text{ mol}^{-1}$ . The a priori bounds on  $\sigma_p^0$  and  $E$  are same for both cases:  $4 \leq \sigma_p^0 \leq 10 \text{ GPa}$  and  $10 \leq E \leq 1000 \text{ kJ mol}^{-1}$ . Mean estimates on model parameters are reported, along with their one standard deviation, for different combinations of exponents  $p$  and  $q$ . Normalized misfit ( $\chi_s^2/N$ ) is also given, where  $N$  is the number of data. Parameter  $\sigma_p^0$  is the Peierls stress at ambient pressure in GPa,  $E$  and  $V$  are activation energy in  $\text{kJ mol}^{-1}$  and volume in  $\text{cm}^3 \text{ mol}^{-1}$ , respectively, and  $A$  is the scaling coefficient in  $\text{s}^{-1} \text{ MPa}^{-2}$ . Note that the activation volumes in the first bound (a) are reported after being multiplied by  $10^4$ , and their mean values are all essentially zero, being less than  $10^{-3} \text{ cm}^3 \text{ mol}^{-1}$ . <sup>a</sup>The shape of the posterior probability distribution for  $V$  is not Gaussian (Figure 1f); therefore,  $1\sigma$  error about mean is not symmetric. Nevertheless, we report the mean  $\pm 1\sigma$  of the distribution because of the extremely tight constraints imposed by data at  $V \sim 0$ .

### 3. Inversion Results

Mei et al. (2010) conducted deformation of olivine under high-pressure (4–9 GPa), low-temperature (673–1273 K), and dry conditions to investigate the low-temperature plasticity regime. Data uncertainties were reported as follows:  $\delta\dot{\epsilon} = 1\%$ ,  $\delta T = 10 \text{ K}$ , and  $\delta\sigma = \delta P = 50 \text{ MPa}$ . In the original study, data were modeled by the flow law with zero  $V$  and constant  $\sigma_p$ . We analyze the same data, along with the reported uncertainties, with the comprehensive flow law for low-temperature plasticity (equation (1)) using all combinations of  $(p, q)$  mentioned in section 2. We excluded four runs, San 154, 155, 167, and 178, from our analysis because pressure was reported to fluctuate during these runs. We ran  $10^6$  MCMC iterations and randomized data at every 100 iterations. The first  $10^4$  models were discarded from the MCMC output to ignore models with too large misfits, and the final output was resampled at an interval of 100 because the autocorrelation function was found to become insignificant at this lag (Figure S1 in the supporting information). The consistency of our MCMC simulations was confirmed by comparing the outcome of five parallel simulations for the given data, where each simulation was initiated using a different starting model. All parallel runs yielded nearly identical values of model parameters (Figure S2). Our inversion results are summarized in Table 1 (case (a)).

Our results indicate that different combinations of  $(p, q)$  yield distinct sets of flow law parameters, and that, for each of these combinations, all parameters are tightly constrained. Significant correlation is observed only between  $E$  and  $A$ , which are almost completely negatively correlated to each other (Table S1a). Note that normalized  $\chi_s^2$  is very large in all cases, and this may be a consequence of underestimating data uncertainties. In recent high-pressure experiments, differential stresses are measured on different crystallographic planes using in situ synchrotron X-ray diffraction, and the average stress over all planes is usually assumed to be the macroscopic stress acting on the polycrystalline sample. Lack of a theoretical basis that can accurately relate microscopic to macroscopic stresses (Karato, 2009) could introduce large discrepancies between the reported

and the “true” magnitudes of macroscopic stress. These uncertainties are not accounted for in the reported errors but could be responsible for the large misfits between deformation data and flow law predictions.

The activation volume is found to be tightly constrained near its lower a priori bound, that is, near zero, for all cases. This suggests that data could favor even lower  $V$ . To test this possibility, we repeated inversion with wider a priori bounds on  $V$ , that is,  $-40 \leq V \leq 40 \text{ cm}^3 \text{ mol}^{-1}$ . A summary of these results (Table 1, case (b)) shows that  $V$  is constrained to below zero for all combinations of  $(p, q)$  without significantly altering our previous estimates on other model parameters (Table 1, case (a)). A physical interpretation of this outcome is difficult because theoretical considerations usually suggest  $V > 0$  for the motion of dislocations in olivine, that is, an increase in pressure is expected to retard deformation in olivine. Indeed, Kawazoe et al. (2009) and Proietti et al. (2016) have suggested positive values of  $V$  for low-temperature plasticity in contrast to our results in Table 1 (case (b)). However, some special cases could result in negative  $V$  for a single slip system, for example, the locking-unlocking mechanism in screw dislocations (Courret and Caillard, 1991; cf. Nabarro, 1997). It is possible that our results indicate such a mechanism underlying low-temperature plasticity. Synthetic tests confirm that negative  $V$  is not an artifact of our MCMC algorithm (see Text S3). Our MCMC inversion can also reproduce the published results of Mei et al. (2010) if the same model equation is assumed (see Text S4), further supporting the reliability of our inversion algorithm. Negative  $V$  may also result from the underestimation of data uncertainties.

Finally, we find that all models yield similar misfits to data, suggesting that all combinations of  $(p, q)$  considered here can explain observed strain rates comparably. Though the misfit is nominally smallest for the case of (1/2, 2) (Table 1, case (a)), it is not very meaningful to prefer it given that misfits are generally very large ( $\chi^2_s/N \gg 1$ ). It is thus difficult to choose a preferred model based on the experimental data of Mei et al. (2010). As a representative case, the model prediction with exponents (1/2, 2) is compared with observed strain rates in Figures 1a–1c. The a posteriori probability distributions of flow law parameters obtained in this case are shown in Figures 1d–1f. Though we have focused on the data of Mei et al. (2010) in this study, the reanalysis of other data is unlikely to improve the situation (see Text S5 for our reanalysis of the data reported in the widely cited study of Evans and Goetze (1979) and Text S6 for our assessment of more recent data).

#### 4. Geophysical Significance of Our Results

Our MCMC inversion results indicate that experimental data of Mei et al. (2010) cannot distinguish between different combinations of  $(p, q)$  in the flow law for low-temperature plasticity. This is consistent with the findings of Frost and Ashby (1982) and Karato, (2008, chap. 9) that suggest that any choice of the exponents  $(p, q)$  yields similar model predictions under experimental conditions if  $0 \leq p \leq 1$  and  $1 \leq q \leq 2$ . Geological strain rates ( $\sim 10^{-15} - 10^{-14} \text{ s}^{-1}$ ) are, however, smaller than laboratory strain rates ( $\sim 10^{-5} \text{ s}^{-1}$ ) by many orders of magnitude, and flow law parameters corresponding to different  $(p, q)$  pairs may yield divergent predictions when extrapolated to geological conditions.

The yield stress of oceanic lithosphere changes with depth due to variation in temperature and pressure. Brittle deformation dominates in shallow lithosphere, and brittle strength increases up to the depth of brittle-plastic transition, beyond which plastic flow dominates (Kohlstedt et al., 1995). In the plastic regime, the effect of temperature is greater than that of pressure, and lithospheric strength decreases with depth. We use our mean flow law parameters for low-temperature plasticity (Table 1, case (a)) to predict the yield stress under the plastic regime (Figure 2). Based on the covariance between flow law parameters (Table S1), we perturb our mean estimates within their associated uncertainties to produce an ensemble of correlated models for low-temperature plasticity (cf. Mullet et al., 2015, section 6.3). The range of yield stresses predicted by this model ensemble is used to estimate 90% confidence intervals about mean predictions. These intervals are shown in Figure 2 for the cases of exponents (1,1) and (1/2, 2).

The strength of the lithosphere is found to vary substantially with the choice of exponents  $(p, q)$  for low-temperature plasticity. For example, the exponents (1, 1) predict the brittle-plastic transition to occur at a depth of  $\sim 27$  km and correspond to a peak strength of 850 MPa. Yield stress declines rather rapidly with depth below the transition for this case. In contrast, if low-temperature plasticity is modeled with exponents (1/2, 2), the brittle regime extends to  $\sim 34$  km depth, and the yield stress exceeds 1 GPa at the brittle-plastic transition. Additionally, the strength decreases only gradually with depth below the transition for this model because of higher activation energy of low-temperature plasticity, and the deformation regime soon transitions into dislocation creep. For diffusion or dislocation creep, a more gradual variation in yield stress is accompanied

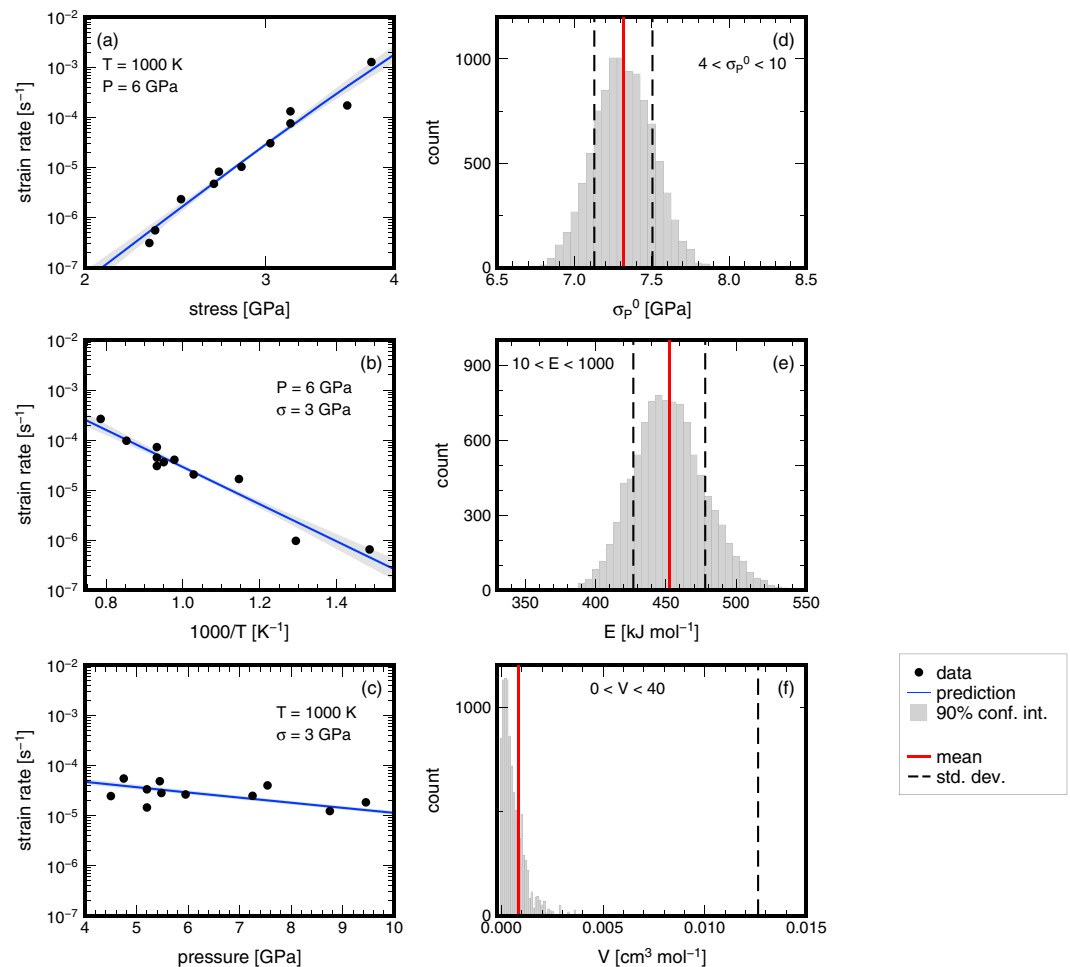


**Figure 1.** Results of MCMC inversion of data of Mei et al. (2010) for the flow law for low-temperature plasticity with exponents  $p = 1/2$  and  $q = 2$ . The fit to observed data in the strain rate versus (a) stress, (b)  $1000/T$ , and (c) pressure. Conditions to which observed strain rates (solid circles) have been normalized are denoted in each panel. Uncertainty of strain rate (1%) is smaller than the size of symbol. Model predictions from equation (1) are shown by blue lines. Grey shaded regions denote 90% confidence intervals about mean model predictions. Panels A posteriori probability distribution of (d) the Peierls stress  $\sigma_p^0$  in gigapascal, (e) activation energy  $E$  in  $\text{kJ mol}^{-1}$ , and (f) activation volume  $V$  in  $\text{cm}^3 \text{mol}^{-1}$ . The a priori bounds on each model parameter are annotated in the respective panels. Mean (solid red) of each a posteriori distribution with the associated  $\pm 1\sigma$  bounds (black dashed line) is also shown. Note that the shape of the a posteriori probability distribution for  $V$  (Figure 1f) is not Gaussian, and therefore, the  $1\sigma$  bounds about mean are not symmetric. Nevertheless, we use the mean  $\pm 1\sigma$  of the distribution because data imposes extremely tight constraints at  $V \sim 0$ .

with lower activation energy (e.g., Cadio and Korenaga, 2016, Figure 5), and the opposite behavior seen here is owing to the pressure term within the exponential function (equation (1)). Yield stress envelopes predicted by other combinations of  $(p, q)$  lie between these two cases.

Our results indicate that different assumptions on the exponents  $(p, q)$  for low-temperature plasticity indeed lead to vastly different predictions for the yield stress envelope of oceanic lithosphere. Because the peak stress associated with all of our models is likely to exceed the critical strength for plate tectonic convection (e.g.,  $\sim 0.2$  GPa) (Richards et al., 2001), these strength profiles underscore the importance of efficient weakening mechanisms.

So far, proposed mechanisms that could potentially reduce the yield strength include semibrittle behavior arising from the interaction of cracks and dislocations (Karato, 2008, chap. 7), shear localization due to grain size reduction and Zener pinning (e.g., Ricard and Bercovici, 2009), and deep thermal cracking (Korenaga, 2007). The potential roles of these mechanisms rest on the strength profile of oceanic lithosphere, and different exponents  $(p, q)$  for low-temperature plasticity would favor different weakening mechanisms.

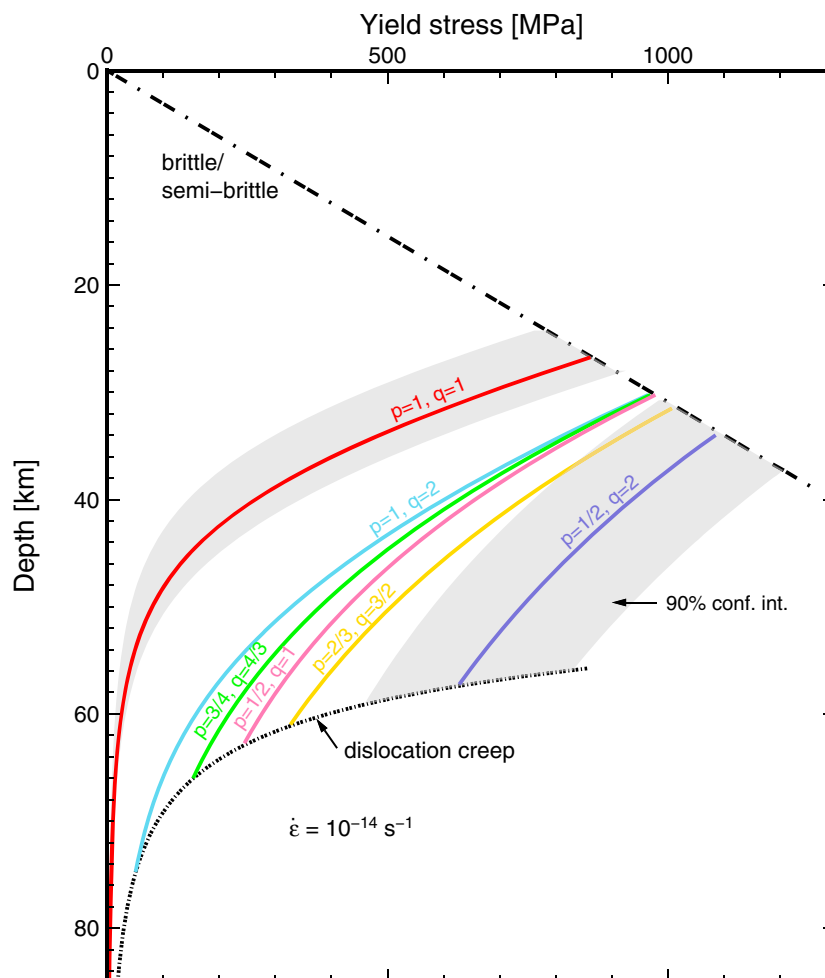


**Figure 2.** The yield stress envelope predicted for dry 100 Ma old oceanic lithosphere. Average density of oceanic lithosphere is assumed to be  $3,300 \text{ kg m}^{-3}$ . Geotherm is based on a half-space cooling model with thermal diffusivity of  $10^{-6} \text{ m}^2 \text{ s}^{-1}$  and surface and mantle potential temperatures of 273 K and 1623 K, respectively. The brittle to plastic transition is marked by the Goetze criterion (black dashed line) (Kohlstedt et al., 1995). Solid curves represent yield stress for plastic flow modeled by low-temperature plasticity that includes all pressure effects (equation (1)). Different colors correspond to different combinations of exponents ( $p$ ,  $q$ ). Mean values of all flow law parameters (Table 1, case (a)) are used to evaluate stress due to low-temperature plasticity at the geological strain rate of  $10^{-14} \text{ s}^{-1}$ . The 90% confidence intervals are shown only for the bounding cases (i.e., exponents (1/2, 2) and (1,1)) for clarity. Predictions for dislocation creep (black dotted) form the lower bound on the strength envelope in the plastic regime. Flow law parameters for dislocation creep are taken from Hirth and Kohlstedt (2003): scaling coefficient,  $A_d=10^{5.04}$ ; stress exponent,  $n=3.5$ ; activation energy,  $E_d=530 \text{ kJ mol}^{-1}$ ; and activation volume,  $V_d=17 \text{ cm}^3 \text{ mol}^{-1}$ .

For example, thermal cracking could substantially damage the lithosphere only down to  $\sim 30 \text{ km}$  depth (Korenaga, 2007), so if low-temperature plasticity is described by the exponents (1, 1), then thermal cracking alone would be sufficient to weaken the entire lithosphere. If, on the other hand, the exponents (1/2, 2) are more appropriate, additional weakening mechanism becomes necessary to explain the generation of plate tectonics on Earth.

Accurately determining the flow law parameters of low-temperature plasticity is, therefore, critical to understanding the origin of plate tectonics. One way to estimate them is to invert experimental data by including the exponents  $p$  and  $q$  among flow law parameters to be determined. Our MCMC inversion scheme is versatile enough to handle such a high degree of nonlinearity, but, as our results in Table 1 indicate, the currently available data are unable to resolve the exponents. We can perhaps identify some combinations of  $p$  and  $q$  that may be less preferred than others based on theoretical mineral physics. For example, (1, 1) corresponds to a case of discrete-obstacle control (with a particular shape of the obstacle) (Frost and Ashby, 1982, chap. 2).

However, in a material with high Peierls stress, the intrinsic resistance of a dislocation against glide caused by the increase in dislocation energy is likely to dominate. Consequently, we may consider that a case of  $p = q = 1$  is unlikely for olivine, where chemical bonding is strong, and hence, the Peierls stress is relatively large. However, other combinations of  $(p, q)$  are difficult to rule out on theoretical basis because these values depend on the details of the barrier for dislocation motion that are not well understood (Kocks et al., 1975). Alternatively, we can use geophysically derived estimates on lithospheric strength to better constrain the flow law parameters of low-temperature plasticity. In this regard, analyzing seamount loading data with realistic mantle rheology appears to be promising (e.g., Zhong and Watts, 2013). Marine geoid anomalies associated with fracture-zone instabilities can also be exploited to constrain the strength of oceanic lithosphere (Cadio & Korenaga, 2016). Given the vital role played by the lithospheric strength in the evolution of terrestrial planets at large, it will be important to make progress through both experimental and observational efforts.

#### Acknowledgments

This work was sponsored by the National Science Foundation under grant OCE-1417327. This work was also supported in part by the facilities and staff of the Yale University Faculty of Arts and Sciences High Performance Computing Center. Reviews by Associate Editor Jacob Tielke, Lars Hansen, and an anonymous reviewer were helpful to improve the clarity of the manuscript. All of experimental data analyzed in this study are available in Mei et al. (2010), Evans and Goetze (1979), and Long et al. (2011).

#### References

- Cadio, C., & Korenaga, J. (2016). Macroscopic strength of oceanic lithosphere revealed by ubiquitous fracture-zone instabilities. *Earth and Planetary Science Letters*, *449*, 295–301.
- Couret, A., & Caillard, D. (1991). Dissociations and friction forces in metals and alloys. *Journal de Physique III. EDP Sciences*, *1*(6), 885–907.
- Evans, B., & Goetze, C. (1979). The temperature variation of hardness of olivine and its implications for polycrystalline yield stress. *Journal of Geophysical Research*, *84*, 5505–5524.
- Frost, H. J., & Ashby, M. F. (1982). *Deformation-mechanism maps: The plasticity and creep of metals and ceramics*. New York: Pergamon Press.
- Hirth, G., & Kohlstedt, D. L. (2003). Rheology of the upper mantle and the mantle wedge: A view from the experimentalists. In J. Eiler (Ed.), *Inside the subduction factory* (pp. 83–105). Washington, DC: American Geophysical Union.
- Karato, S.-I. (2008). *Deformation of earth materials: Introduction to the rheology of the solid earth*. New York: Cambridge University Press.
- Karato, S.-I. (2009). Theory of lattice strain in a material undergoing plastic deformation: Basic formulation and applications to a cubic crystal. *Physical Review B: Condensed Matter*, *79*(21), 214106. <https://doi.org/10.1103/PhysRevB.79.214106>
- Karato, S.-I., & Jung, H. (2003). Effects of pressure on high-temperature dislocation creep in olivine. *Philosophical Magazine*, *83*, 401–414.
- Karato, S., & Wu, P. (1993). Rheology of the upper mantle: A synthesis. *Science*, *260*, 771–778.
- Kawazoe, T., Karato, S.-I., Otsuka, K., Jing, Z., & Mookherjee, M. (2009). Shear deformation of dry polycrystalline olivine under deep upper mantle conditions using a rotational Drickamer apparatus (RDA). *Physics of the Earth and Planetary Interiors*, *174*, 128–137. <https://doi.org/10.1016/j.pepi.2008.06.027>
- Kocks, W. F., Argon, A. S., & Ashby, M. F. (1975). Thermodynamics and kinetics of slip. *Progress Materials Science*, *19*, 291.
- Kohlstedt, D. L., Evans, B., & Mackwell, S. J. (1995). Strength of the lithosphere: Constraints imposed by laboratory experiments. *Journal of Geophysical Research*, *100*, 17,587–17,602.
- Korenaga, J. (2007). Thermal cracking and the deep hydration of oceanic lithosphere: A key to the generation of plate tectonics? *Journal of Geophysical Research*, *112*, B05408. <https://doi.org/10.1029/2006JB004502>
- Korenaga, J., & Karato, S.-I. (2008). A new analysis of experimental data on olivine rheology. *Journal of Geophysical Research*, *113*, B02403. <https://doi.org/10.1029/2007JB005100>
- Liu, W., Kung, J., & Li, B. (2005). Elasticity of San Carlos olivine to 8 GPa and 1073 K. *Geophysical Research Letters*, *32*, L16301. <https://doi.org/10.1029/2005GL023453>
- Long, H., Weidner, D. J., Li, L., Chen, J., & Wang, L. (2011). Deformation of olivine at subduction zone conditions determined from in situ measurements with synchrotron radiation. *Physics of the Earth and Planetary Interiors*, *186*, 23–35. <https://doi.org/10.1016/j.pepi.2011.02.006>
- Mei, S., Suzuki, A. M., Kohlstedt, D. L., Dixon, N. A., & Durham, W. B. (2010). Experimental constraints on the strength of the lithosphere. *Journal of Geophysical Research*, *115*, B08204. <https://doi.org/10.1029/2009JB006873>
- Mullet, B. G., Korenaga, J., & Karato, S.-I. (2015). Markov chain Monte Carlo inversion for the rheology of olivine single crystals. *Journal of Geophysical Research: Solid Earth*, *120*, 3142–3172. <https://doi.org/10.1002/2014JB011845>
- Nabarro, F. R. N. (1997). Fifty-year study of the Peierls-Nabarro stress. *Materials Science and Engineering A*, *234*, 67–76.
- Proietti, A., Bystricky, M., Guignard, J., Bejina, F., & Crichton, W. (2016). Effect of pressure on the strength of olivine at room temperature. *Physics of the Earth and Planetary Interiors*, *259*, 34–44.
- Raterron, P., Wu, Y., Weidner, D. J., & Chen, J. (2004). Low-temperature olivine rheology at high pressure. *Physics of the Earth and Planetary Interiors*, *145*, 149–159.
- Ricard, Y., & Bercovici, D. (2009). A continuum theory of grain size evolution and damage. *Journal of Geophysical Research*, *114*, B01204. <https://doi.org/10.1029/2007JB005491>
- Richards, M. A., Yang, W.-S., Baumgardner, J. R., & Bunge, H.-P. (2001). Role of a low-viscosity zone in stabilizing plate tectonics: Implications for comparative terrestrial planetology. *Geochemistry, Geophysics, Geosystems*, *2*, 1,026.
- Solomatov, V. S. (1995). Scaling of temperature- and stress-dependent viscosity convection. *Physics of Fluids*, *7*, 266–274.
- Zhong, S., & Watts, A. B. (2013). Lithospheric deformation induced by loading of the Hawaiian Islands and its implications for mantle rheology. *Journal of Geophysical Research: Solid Earth*, *118*, 6025–6048. <https://doi.org/10.1002/2013JB010408>